

Multi-differential $\nu_\mu - {}^{40}\text{Ar}$ charged current interactions with no pions in the final state with the MicroBooNE detector

Introduction

In neutrino interactions with heavy elements, the nuclear modeling is not well understood.

→ As a consequence, not directly observed variables (for instance, E_ν) are not accurately estimated.

Main contributions are:
 ▶ final-state interactions (FSI)
 ▶ Fermi motion
 ▶ multinucleon correlation effects

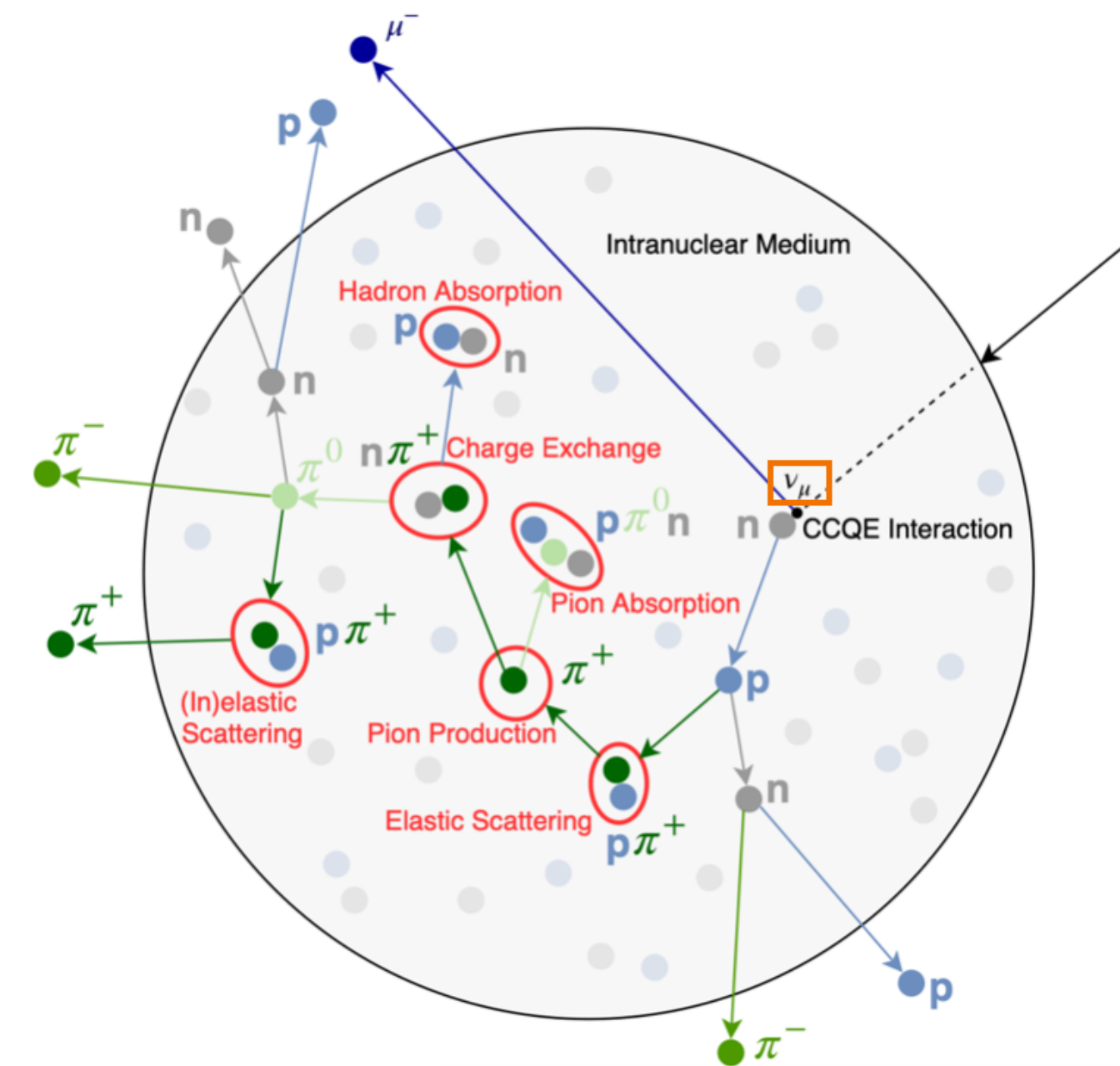


Figure 1: Illustration of FSI in a charged current (CC) quasi-elastic scattering of ν_μ with ${}^{40}\text{Ar}$. Figure adapted from [1].

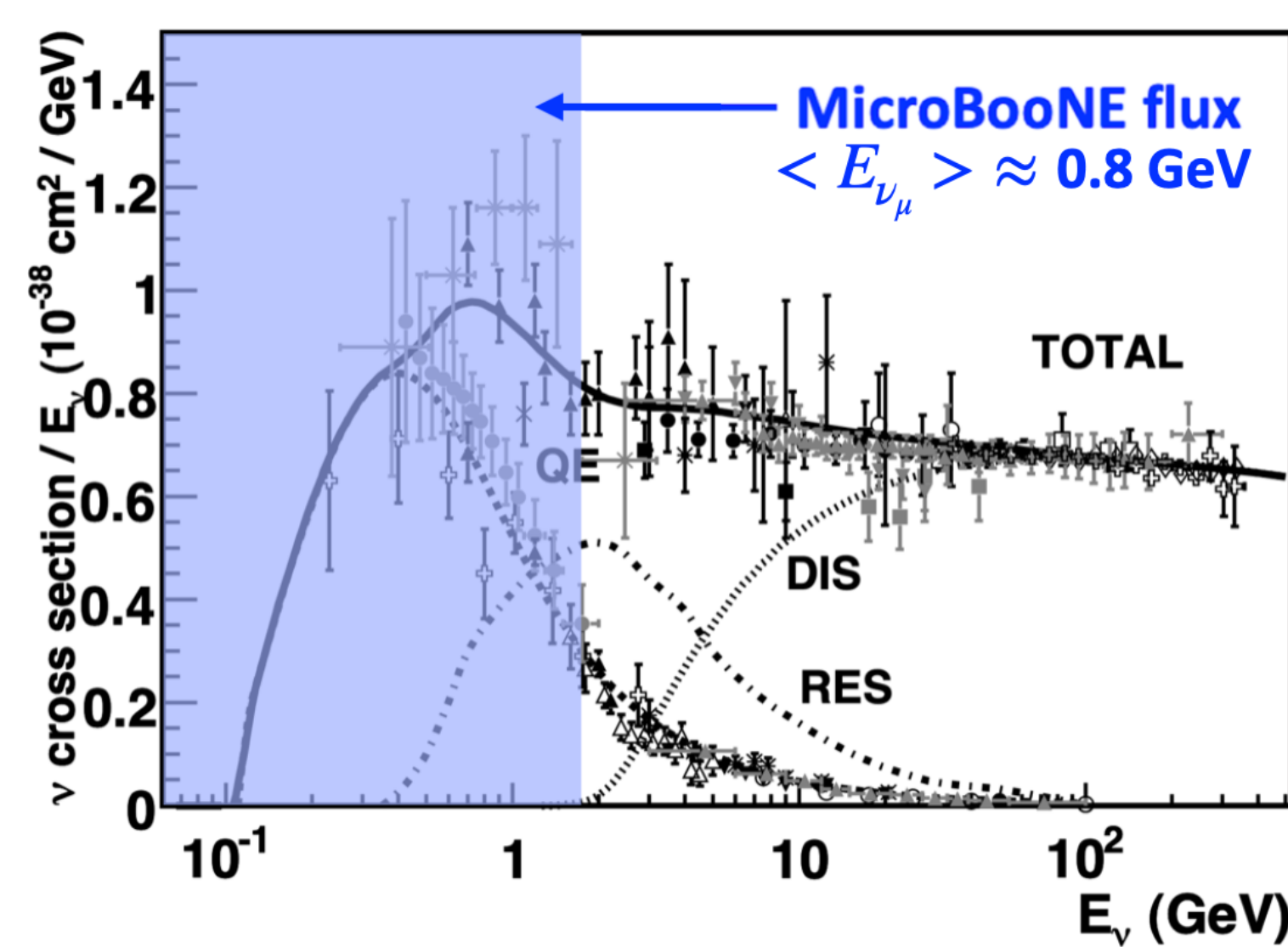


Figure 2: Total ν per nucleon CC cross sections per E_ν . In MicroBooNE, the quasi-elastic process is the most dominant interaction. Figure adapted from [2].

$CC0\pi$ is an exciting channel because:

- ❖ transverse kinematic imbalance variables, which are sensitive to nuclear effects, can be studied
- ❖ it can help to connect cross section models between oscillation experiments with different nuclear targets

The MicroBooNE detector operated from 2015 to 2021, accumulating the largest dataset of $\nu_\mu - {}^{40}\text{Ar}$ CC interactions.

Signal Definition

- $0.1 \text{ GeV}/c \leq p_\mu \leq 1.2 \text{ GeV}/c$
- the final state contains:
 - ▶ at least one proton
 - ▶ no mesons and antimesons
- $0.25 \text{ GeV}/c \leq p_{p\text{leading}} \leq 1. \text{ GeV}/c$

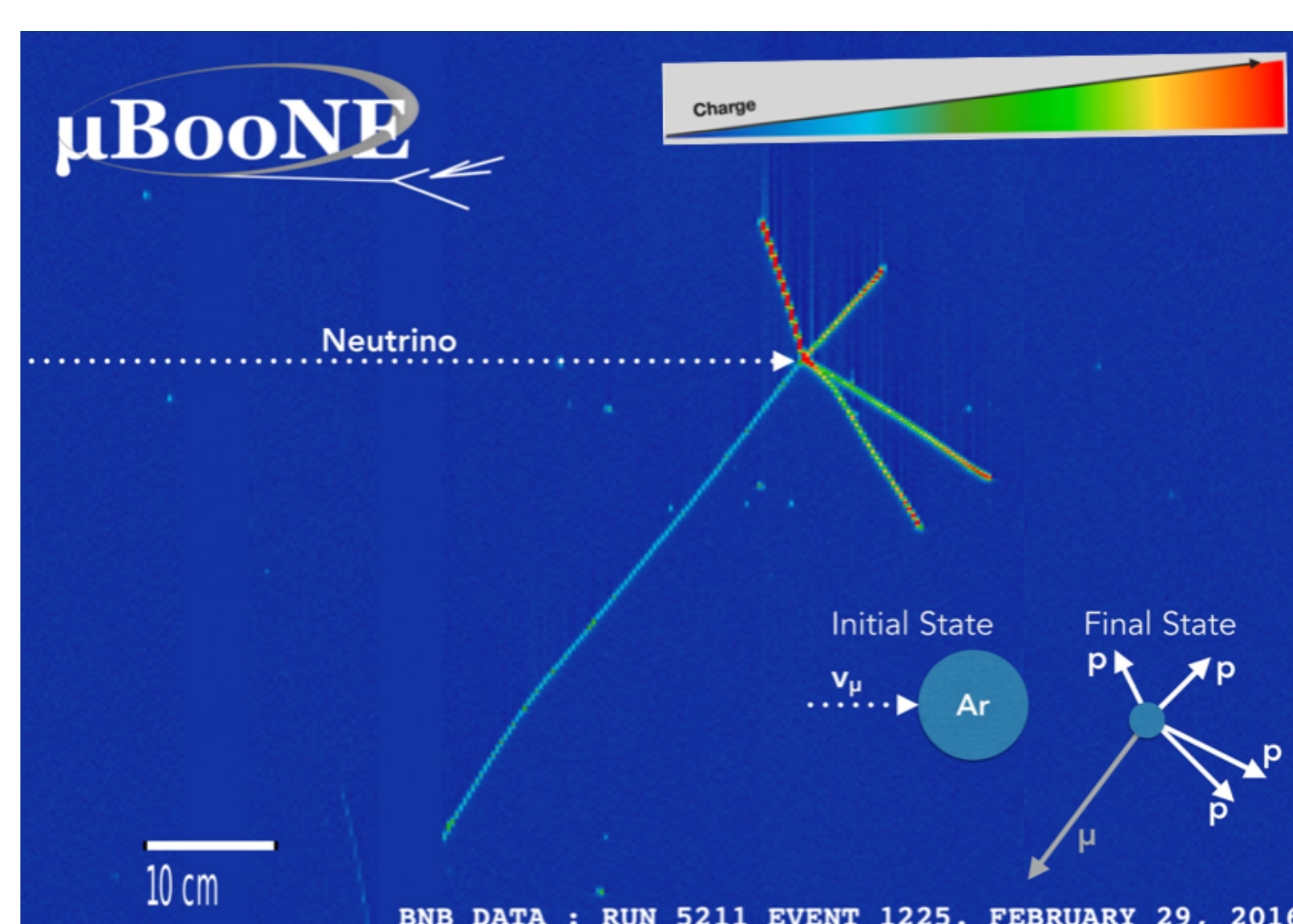


Figure 3: A MicroBooNE event display which includes reconstructed μ and p candidates.

Kinematic Imbalance Variables

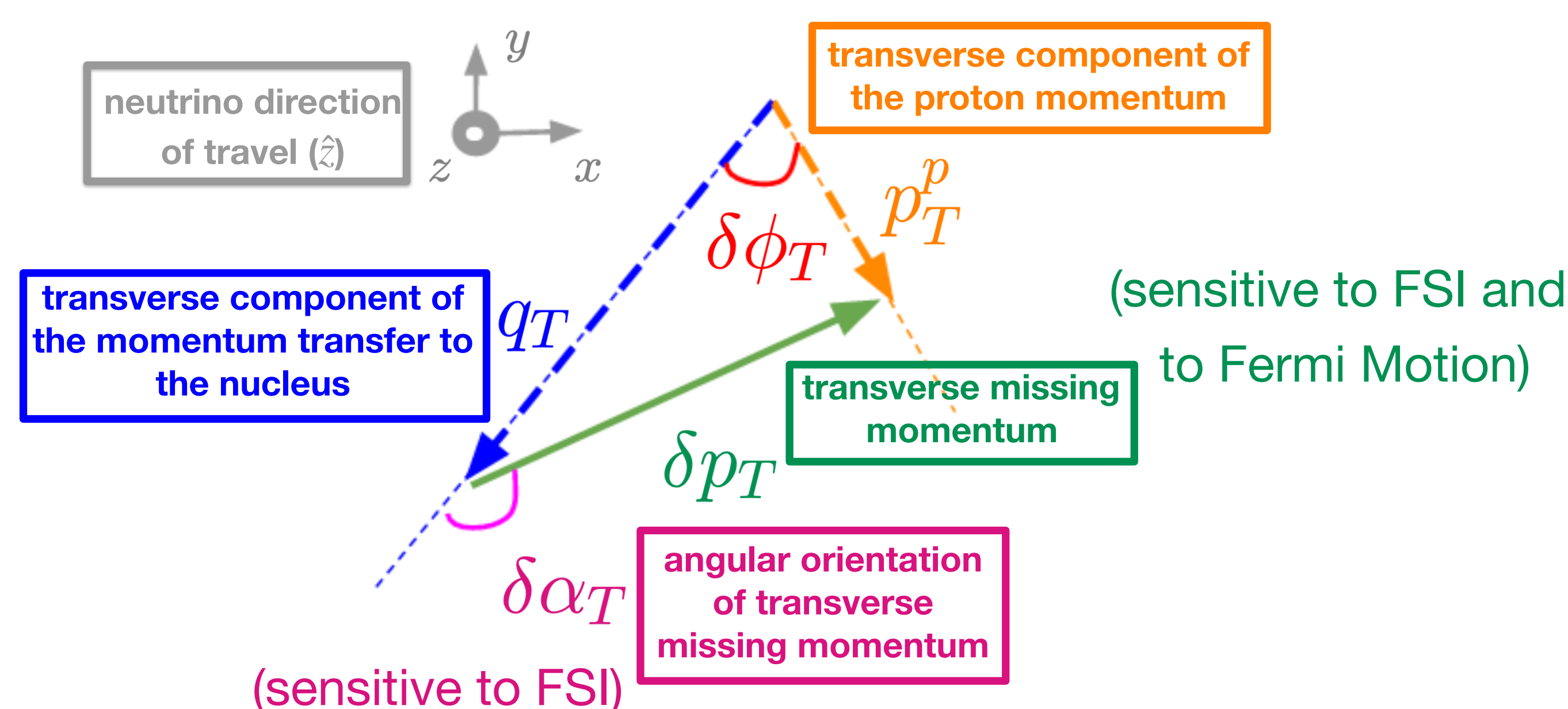


Figure 4: Representation of the kinematic imbalance variables on the transverse plane. Figure adapted from [3].

Results

We present flux-integrated multi-differential cross sections [4]. Statistical (shape-only systematic) uncertainties are included in the inner (outer) error bars. The remainder of the total uncertainty is shown by the gray band along the x-axis.

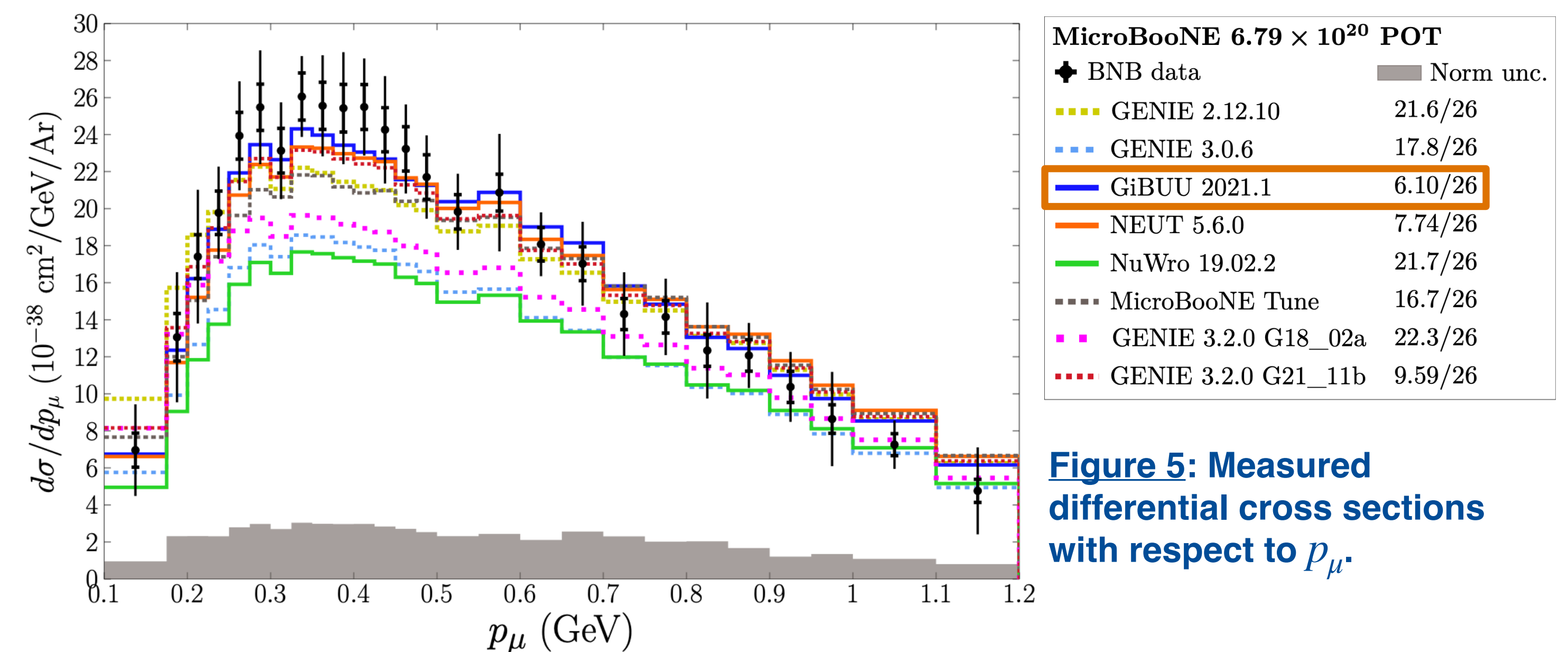


Figure 5: Measured differential cross sections with respect to p_μ .

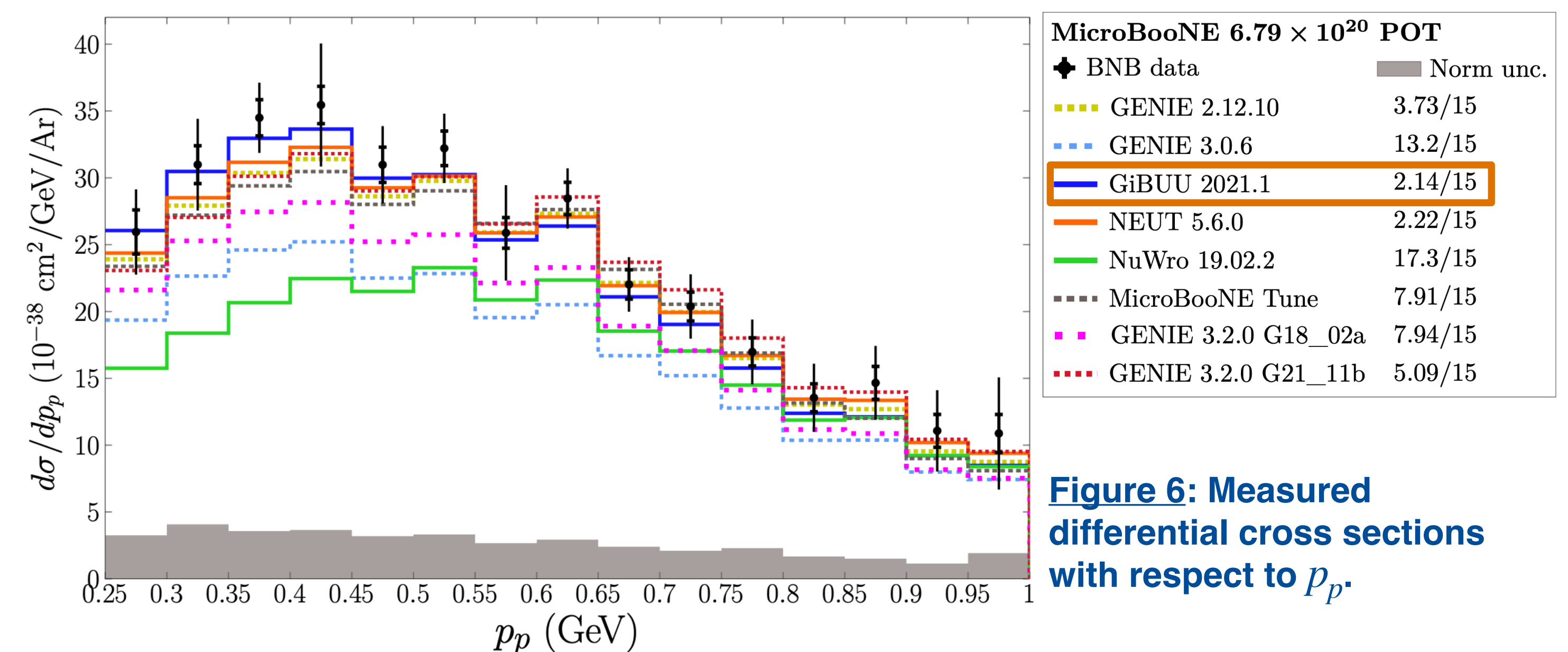


Figure 6: Measured differential cross sections with respect to p_P .

- ➔ The GIBUU 2021.1 model achieves the best level of agreement with data.
- ➔ At moderate p_μ and at low p_P , the measured cross-sections are noticeably larger than the predicted ones. In these regions, the NuWro 19.02.2 model significantly underpredicts.

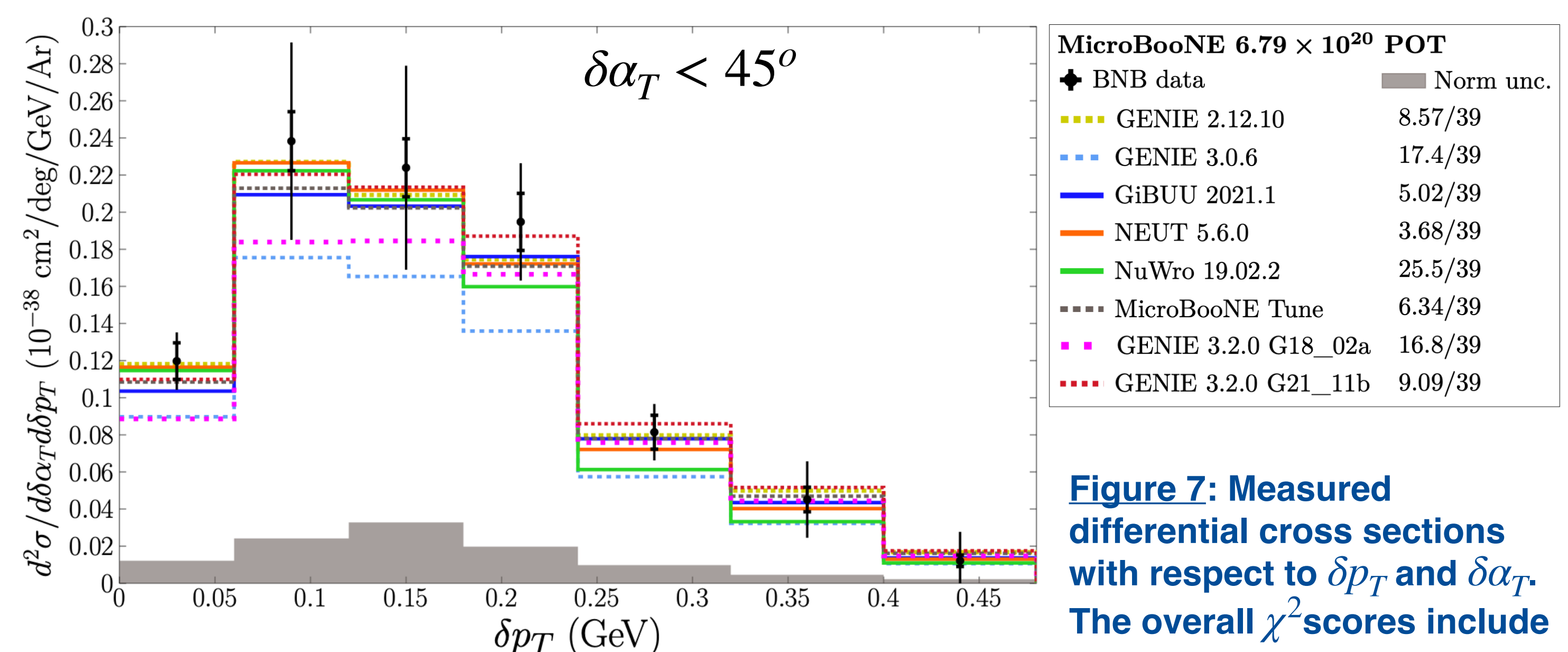
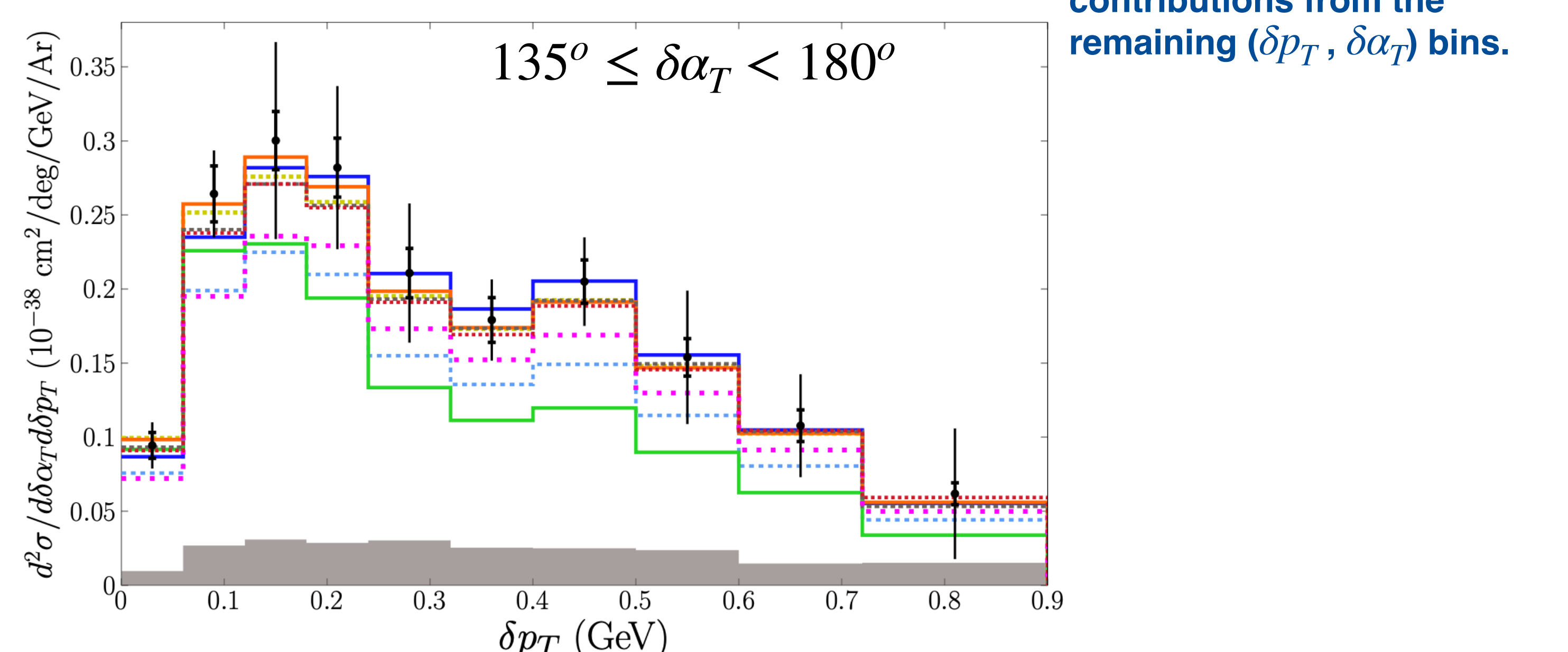


Figure 7: Measured differential cross sections with respect to δp_T and $\delta\alpha_T$. The overall χ^2 scores include contributions from the remaining $(\delta p_T, \delta\alpha_T)$ bins.



- ➔ The NuWro 19.02.2 model agrees well with data at low $\delta\alpha_T$, but diverges at high $\delta\alpha_T$. This concludes that, in this generator, proton FSI are underestimated.

References

- [1] L. Bathe-Peters et al., arXiv:2201.04664 (2022)
- [2] J. A. Formaggio et al., Rev. Mod. Phys. 84, 1307 (2012)
- [3] P. Abratenko et al. (The MicroBooNE Collaboration), Phys. Rev. D 109, 092007 (2024)
- [4] P. Abratenko et al. (The MicroBooNE Collaboration), arXiv:2403.19574v2 (2024)